

# Comparative Annual Energy Yield of Total Cross Tied – in - Series and Conventional PV Array Configuration Under Unshaded and Partial Shading Conditions in Urban Areas

Niti Agrawal\*<sup>‡</sup>, Avinashi Kapoor \*\*, Mridula Gupta\*\*

\* Department of Physics, Shyamlal College, University of Delhi, Delhi-110032, India

\*\* Department of Electronic Science, University of Delhi South Campus, New Delhi- 110021, India  
([nitichin@yahoo.co.in](mailto:nitichin@yahoo.co.in), [avinashi\\_kapoor@yahoo.com](mailto:avinashi_kapoor@yahoo.com), [mridula@south.du.ac.in](mailto:mridula@south.du.ac.in))

<sup>‡</sup>Corresponding Author; Niti Agrawal, Shyamlal College, University of Delhi, Delhi-110032, India,  
Tel: +91 9810391961, [nitichin@yahoo.co.in](mailto:nitichin@yahoo.co.in)

*Received: 27.11.2022 Accepted: 03.01.2023*

**Abstract-** Photovoltaic (PV) technology has great potential for electricity generation in an urban environment. Urban areas are characterised by the presence of high-rise buildings, trees, chimneys and other structures, the shadow of which becomes unavoidable for the installed PV arrays in their neighbourhood. Generally, it is not possible to remove or relocate such structures in the vicinity of the PV system. Such persistent partial shadings can result in a significant loss in the annual energy yield of the PV array. To get the desired energy yield, the installation of more PV modules would be required which implies a higher cost of electricity for the end users. The present work compares the annual energy yield and DC performance ratio of total cross tied in series or TCT-S PV array with the conventional array under unshaded and five partial shaded conditions. The first part of the work comprises experimentally measuring current-voltage curves for both the arrays at different operating temperatures and irradiance in real outdoor conditions for several days. The outdoor data is used to generate 22-element maximum power (P<sub>max</sub>) matrix as per IEC61853-1, for both the arrays under unshaded and partially shaded conditions. The second part of the work comprises numerically estimating the energy yield of both the PV arrays (normalized to 1kW system) under each scenario using their respective P<sub>max</sub> matrix, weather data obtained for one complete year for the location and the translation equations. It is found that a significant enhancement of annual energy yield ranging from 4.8 % to 36.7 % under partial shadings can be obtained by the TCT-S array over the conventional array.

**Keywords** Power matrix, partial shading, total cross tied, annual energy, hybrid array, performance ratio.

## 1. Introduction

Partial Solar Photovoltaics (PV) has gained much popularity owing to the technological advancements, decline in the module prices and public acceptance. For urban areas which are continuously expanding, solar PV has a great potential to supply a substantial share of high energy demands, reduce the carbon emission and achieve sustainability [1]. Rack-mounted Photovoltaics and Building Integrated

Photovoltaics (BIPV) are commonly used PV system in urban areas to generate electricity. A challenging condition faced by the installed PV arrays in such environment which can significantly decrease its energy generation is Partial Shading (PS) [2].

PS is a commonly occurring condition of inhomogeneous distribution of solar irradiance on PV surface [3], [4]. Urban areas are characterised by the presence of high-rise buildings, trees, chimneys, overhead transmission wires and other

structures, the shadow of which becomes unavoidable for the installed PV arrays in the neighbourhood [5], [6]. Self-shading of modules i.e., modules get shaded by the rows of modules in the front, is also almost impossible to avoid in BIPV and in limited roof top spaces [7], [8]. Generally, it is not possible to remove or relocate structures in the vicinity of PV system casting shadow over it. Under such situations, partial shadings are repeated daily and becomes persistent. Such partial shadings can result in significant loss in the annual energy yield of PV array [9]–[13]. In order to get the desired energy yield, installation of more PV modules would be required which implies higher cost of electricity for the end users. Therefore, it is of practical significance to keep exploring different designs of PV arrays which are PS tolerant so that the loss of energy yield can be minimized even when the array is shaded for a long period of time.

A widely discussed approach to increase the shading resilience and hence the performance of partially shaded PV array is to alter the electrical interconnection of cells/modules in a PV array from series to parallel [14]–[18]. Accordingly, many different types of parallel architecture such as series-parallel (SP), total cross tied (TCT), bridge linked (BL), honey comb (HC) have been tested by the researchers to find the optimum configuration under PSCs [19]–[26]. The studies concluded that TCT configuration exhibits superior performance over others under PSCs. Various other configurations, such as hybrid of two configurations [27], [28], mathematical puzzle based [29]–[33] and reconfigured configurations, where main objective is to equalize the generated currents by different electrical rows [34]–[40] have also been investigated. All these strategies have their own advantages and limitations. However, all these studies conducted the comparative analysis of PV array configurations at only one instant of time, at one value of operating temperature and irradiance (generally 25°C and 1000 W/m<sup>2</sup>). However, a PV array in field conditions experience wide range of operating temperature, solar irradiance and partial shading conditions. These previous studies though useful to emphasise the impact of partial shading on these configurations, are insufficient to predict their comparative long-term performance in real field conditions. These studies do not provide information of how much additional energy one configuration can produce in comparison to other over a period of time in real operating conditions under the impact of PSCs. This information is of paramount significance not only from the point of view of solar project developers but also from the end customers. However, the comparative effect of PS on the annual energy yield of different designs of PV modules/arrays has not been focussed much.

The authors in this paper investigate the comparative performance of two different configurations of PV array under uniform irradiance and partial shaded conditions. The two configurations of PV array used are:

- (i) Total-cross-tied in series or TCT-S configuration
- (ii) Conventional series in series or S-S array

The authors in their previous work investigated the instantaneous maximum output power of a partially shaded

TCT-S array in the absence and presence of bypass diodes. [41]. The present work is focussed on the comparative long-term performance of these configurations. The effect of persistent PSCs on their annual energy yield as well as DC performance ratio is investigated and compared.

As the first part of the study, extensive experimental work in real operating conditions of characterising PV arrays under uniform and five partial shading scenarios has been done. The outdoor data is used to generate 22-element maximum power ( $P_{max}$ ) matrix as per IEC61853-1 for both the arrays under unshaded and shaded conditions. The second part of the study comprises of estimating the energy yield of the arrays under different conditions, using the respective  $P_{max}$  matrix, weather data obtained for the year for the location and the translation equations [42]. The details of the methodology used in this study is presented in section 2. The parameters taken into account for estimating energy yield in this work are local solar irradiance, array operating temperature as a function of ambient temperature and wind speed. Comparison of the annual energy yield and DC performance ratio of the TCT-S configuration with the conventional S-S configuration has been conducted to understand the effect of shading on their energy generation.

The present study has relevance if the shaded conditions occur statically for fixed duration of the day as in multi-storeyed complexes in urban environment. The results of the study would benefit the Solar Project Developers to extract maximum energy under persistent partial shading conditions, benefitting the end customers too.

## 2. Methodology

The outline of the methodology used for this study is presented Fig. 1, while the details are presented below:

### *STEP I: Design of PV Array Configurations*

Two different configurations of PV array have been used for this research work, as described below:

**1. Conventional series in series or S-S Array-** This configuration of PV array is formed by connecting S-modules in series. S-module is the one which has 36 solar cells connected in series. The schematic of S-module with its cell interconnections inside is shown in Fig. 2.a.

**2. Total cross tied in series or TCT-S Array-** This configuration is the hybrid of total-cross-tied and series configuration. In this configuration, TCT-modules are connected in series to form the TCT-S PV array. TCT-module is the one which has 36 cells inside interconnected in TCT scheme. and such modules are further interconnected in series. The schematic of TCT-module with its cell interconnections inside is shown in Fig. 2.b.

One bypass diode per module has been used as a protection against the adverse situation like hotspots, in both the PV arrays. Further details of the array design have been presented in our previous paper [41].

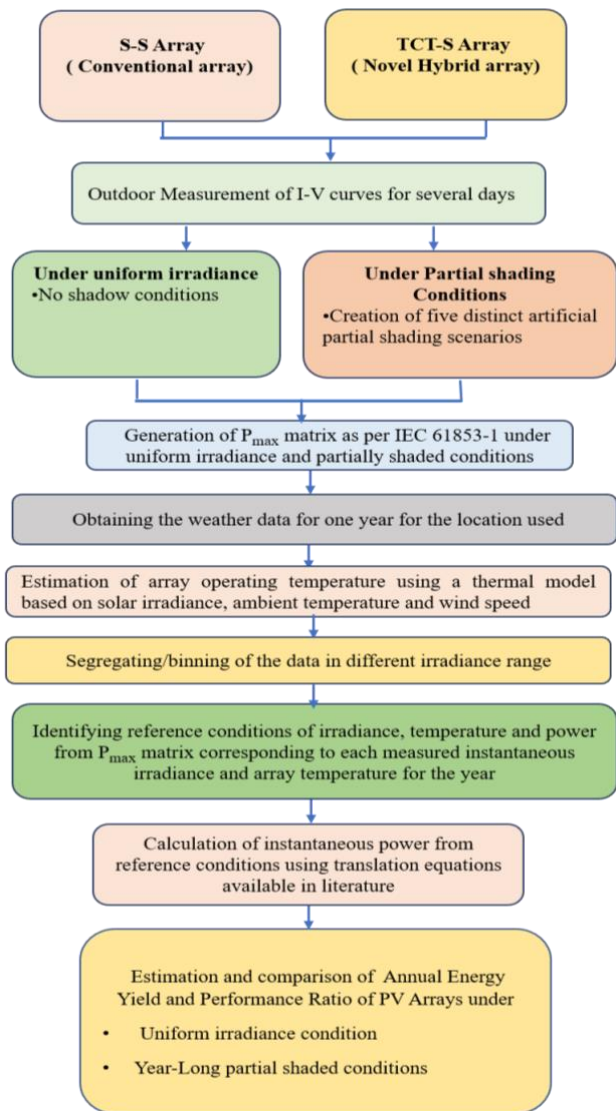


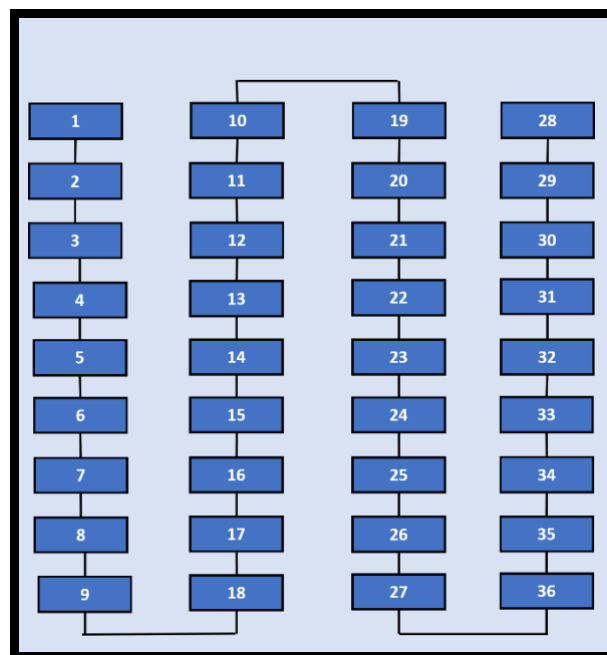
Fig. 1. Representation of the methodology used.

**STEP II: Outdoor Measurements of PV Array Configurations**

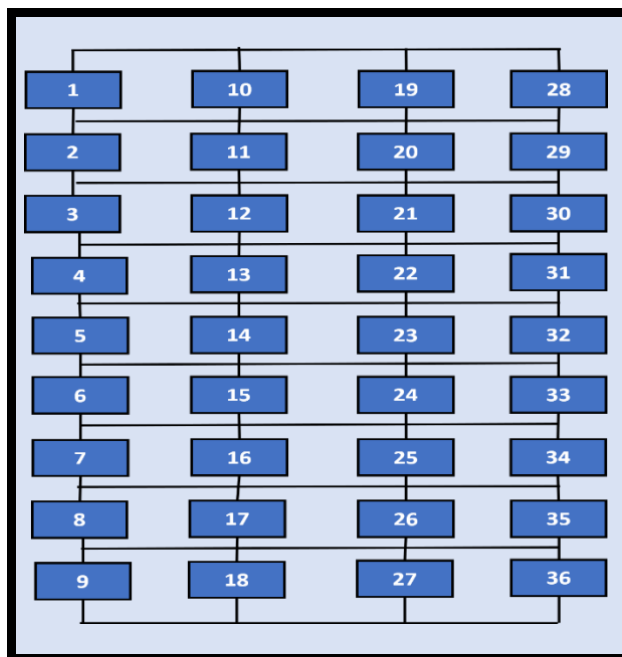
All the measurements for PV arrays are conducted at National Institute of Solar Energy (NISE), Gurugram, Haryana, India. The site has latitude 28.4700° N and longitude 77.0300° E with an elevation of 216 m from sea level. For the outdoor measurements, both the arrays were fixed on rigid structures with a tilt angle 28.5°, facing south. A portable instrument called Solmetric P-V Analyser (PVA-1000S) is used to measure the outdoor current-voltage characteristics of the arrays. The outdoor measurements have been recorded under uniform irradiance and five shading conditions.

**STEP III: Generation of partial shading conditions**

The evaluation and comparison of the energy yield of both the arrays have been done under five partial shading scenarios (shown in Fig. 3). These shading scenarios are inspired by shadings which can occur commonly in urban areas.



(a)



(b)

Fig. 2. Schematic of the (a) S-module (b) TCT-module

Different shading scenarios have been created artificially using three different sheets of paper whose transmissivity was found to be 0%, 42.6% and 61.8% [14]. Consequently, the shade intensity created by these sheets are 100 %, 57.4% & 38.2% respectively.

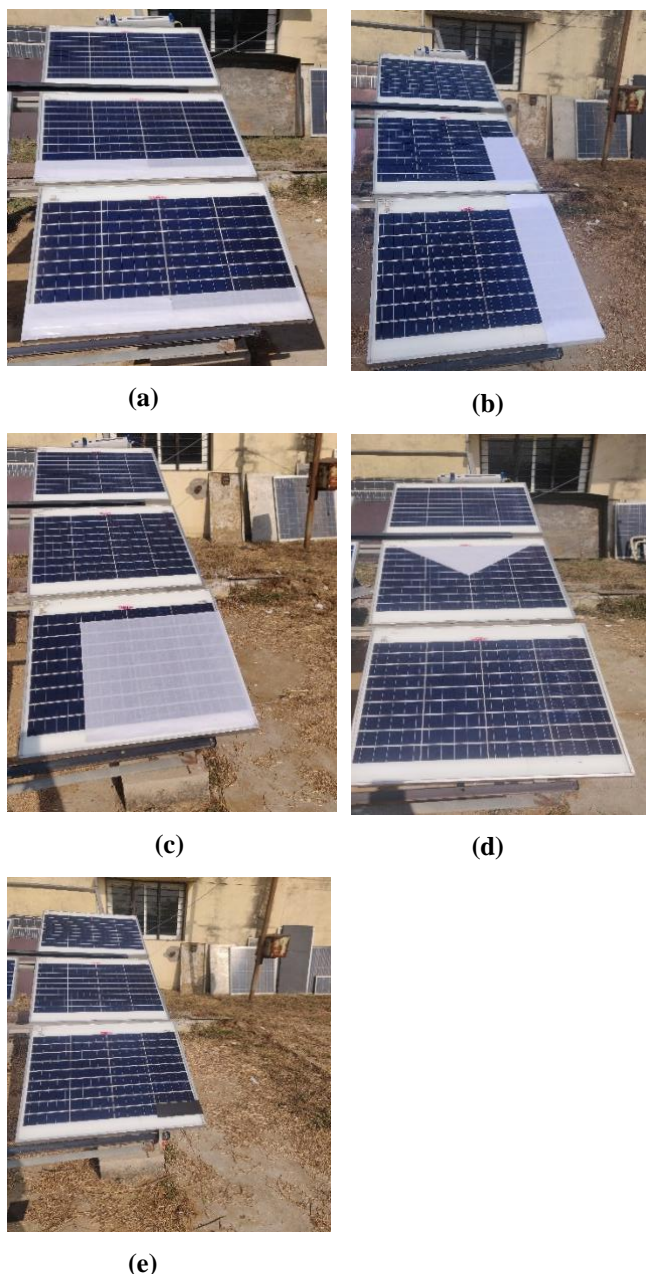


**Fig. 3.** Partial shading scenarios used in this work. (a) scenario 1 (b) scenario 2 (c) scenario 3 (d) scenario 4 (e) scenario 5.

It is important to point out here that the shading conditions considered are static and the variation of shading patterns dimensions with the time of the day/seasons have not been taken into account in the present study. Such simplification was adopted because: 1) it is difficult to cast identical dynamic natural shadow on two separately installed arrays all the time in real operating conditions, 2) Even for artificially generated shadow, changing its dimensions continuously throughout is extremely difficult, 3) the work primarily focusses on the investigating the comparative effect of persistent shadings on energy generation capabilities of the conventional and proposed configuration.

Brief description of the shading scenarios considered in this study is given below:

**Shading Scenario 1:** In this scenario, one row each of the two PV modules within the array was shaded unevenly with shading intensity 57.4% and 38.2% (Fig. 3.a). This scenario is inspired by the self-shading of PV array where in modules can get shaded row wise by the modules present in front of them.

**Shading Scenario 2:** In this scenario, column wise shading was considered (Fig. 3.b). Such a shading can arise due to the presence of any nearby structure e.g., chimney which can partially shade the array column wise. The shading intensity used is 57.4%.

**Shading Scenario 3:** In this scenario, a portion of one PV module within the array was shaded (24 cells out of 36) with intensity 38.2% (Fig. 3.c). This scenario is inspired by the situation especially for the BIPV or roof top installed arrays, where the shadow from a nearby big tree can obstruct the incident solar irradiance on some portion of the PV array.

**Shading Scenario 4:** In this scenario, a triangular shading of intensity 57.4% was considered on a single module within the array (Fig. 3.d). This scenario is inspired by the situation, where the edge of a nearby building cast shadow on some part of the PV array surface.

**Shading Scenario 5:** In this shading scenario only a single cell within the entire array was shaded with 100 % intensity (Fig. 3.e). This situation represents any condition such as complete irradiance obstruction or a faulty/cracked cell, due to which a single cell within the array ceases to generate any power.

**STEP IV: Generation of Power Matrix**

The several days outdoor I-V data for both the arrays under uniform irradiance condition and shading scenarios, obtained using Solmetric P-V Analyser, is used to generate the 22-element  $P_{max}$  matrix in accordance with IEC61853-1[43]. The 22 conditions of different temperature and irradiance used in  $P_{max}$  matrix is shown in Table 1.

**Table 1.**  $P_{max}$  at 22 sets of Irradiance and Temperature Conditions as per IEC 61853-1 standard.

$P_{max}$ Versus Irradiance and Temperature	
Irradiance (W/m <sup>2</sup> )	Module Temperature (°C)

	15	25	50	75
100	1	2	NA	NA
200	3	4	NA	NA
400	5	6	7	NA
600	8	9	10	11
800	12	13	14	15
1000	16	17	18	19
1100	NA	20	21	22

Elements of such a matrix are the values of maximum power obtained by the array at these 22 conditions of temperature and irradiance. Six matrices each for both the arrays, corresponding to uniform irradiance condition and shading scenarios 1-5 were generated.

**STEP V: Obtaining Weather Data**

The weather data for the site which is National Institute of Solar Energy (NISE), Haryana, India, for one complete year is obtained. The details of the weather data are presented in [42]. The data of local solar irradiance (G), ambient temperature (T) and wind speed (WS) is recorded after every 10 minutes. Details of weather station is as follows:

Name of equipment	Make & model no.
Pyranometer	EKO, MS-802
Wind sensor	Young, 05103
Temperature sensor	Vaisala, HMP 155

**STEP VI: Estimating PV Array Operating Temperature**

Based on the local environmental conditions of solar irradiance, ambient temperature and wind speed, array's operating temperature is estimated by an empirically based thermal model [44] which is given by equation (1).

$$T_a = G(e^{a+b*WS}) + T \tag{1}$$

where:

$T_a$  = Back-surface array temperature, (°C).

$T$  = Ambient air temperature, (°C)

$G$  = Solar irradiance incident on module surface, (W/m<sup>2</sup>)

$WS$  = Wind speed measured at standard 10-m height, (m/s)

$a = -3.56$ , an empirically-determined coefficient establishing the upper limit for array temperature at low wind speeds and high solar irradiance

$b = -0.0750$ , also an empirically-determined coefficient establishing the rate at which module temperature drops as wind speed increases.

**STEP VII: Segregating Data in Different Irradiance Bins**

The obtained yearly data is segregated in the following seven irradiance bins corresponding to seven irradiance conditions mentioned in  $P_{max}$  matrix:

1	$G \leq 150 \text{ W/m}^2$
2	$150 \text{ W/m}^2 < G \leq 250 \text{ W/m}^2$
3	$250 \text{ W/m}^2 < G \leq 450 \text{ W/m}^2$
4	$450 \text{ W/m}^2 < G \leq 650 \text{ W/m}^2$
5	$650 \text{ W/m}^2 < G \leq 850 \text{ W/m}^2$
6	$850 \text{ W/m}^2 < G \leq 1020 \text{ W/m}^2$
7	$G > 1020 \text{ W/m}^2$

**STEP VIII: Identifying Reference Conditions of Irradiance, Temperature and Power Corresponding to the Weather Data**

For estimating the instantaneous power generated by any array under any particular scenario i.e., uniform irradiance or any one of the considered shading scenario, the experimentally generated  $P_{max}$  matrix by the array under that scenario is selected. Corresponding to each measured value of irradiance and array temperature, reference conditions of irradiance, temperature and power are identified from the  $P_{max}$  matrix generated under the respective scenario. The same is illustrated below using the example of TCT-S array under uniform irradiance condition.

**Table 2.**  $P_{max}$  matrix obtained for TCT-S array (normalized to 1kW) under uniform irradiance for 22 different irradiance and temperature

$P_{max}$ Versus Irradiance and Temperature for TCT-S array under uniform irradiance condition	
Irradiance (W/m <sup>2</sup> )	Temperature (°C)

	15	25	50	75
100	85.5	86.8	NA	NA
200	202.6	199.4	NA	NA
400	434.6	425.2	391.6	NA
600	642.5	620.9	564.9	503.9
800	835.8	805.9	729.1	649.1
1000	1040.9	1000.0	897.7	795.3
1100	NA	1097.2	985.9	869.6

The  $P_{max}$  matrix obtained experimentally for TCT-S array under uniform irradiance conditions is presented in Table 2. These 22 conditions of maximum power obtained experimentally (in W) at seven different conditions of irradiance and four different temperatures work as the reference conditions for all the measured conditions of irradiance and array temperature for the year (obtained using weather station). For example, if any measured weather condition of irradiance (G) and array temperature ( $T_a$ ) is 853.5  $W/m^2$  and 41.1°C respectively, it lies in the bin 6 i.e., falling in the irradiance range greater than 850  $W/m^2$  and less than or equal to 1000  $W/m^2$ . For such a set of G and  $T_a$ , the reference condition of irradiance ( $G_{ref}$ ) is 1000  $W/m^2$  and temperature ( $T_{ref}$ ) is 50°C (closest to  $T_a$ ). The experimentally found power at these conditions is 897.7 W (highlighted in yellow in  $P_{max}$  matrix). This becomes the reference power ( $P_{ref}$ ) for the instantaneous condition of 853.5  $W/m^2$  and 41.1°C. For the entire weather data, reference conditions of  $G_{ref}$ ,  $T_{ref}$  and  $P_{ref}$  are identified from the obtained  $P_{max}$  matrix.

**STEP IX: Estimation of Instantaneous Power Corresponding to the Weather Data**

After identifying the reference conditions for the yearlong measured data of irradiance and array temperature (every 10 minutes), instantaneous power output,  $P_o$  corresponding to these conditions is estimated using the following translation equations [45]:

For  $G > 125 W/m^2$ ,

$$P_o = \left(\frac{G}{G_{ref}}\right) * P_{ref} * ((T_a - T_{ref}) * \gamma + 1) \quad (2)$$

For  $G \leq 125 W/m^2$ ,

$$P_o = \left(\frac{G^{2*0.008}}{G_{ref}}\right) * P_{ref} * ((T_a - T_{ref}) * \gamma + 1) \quad (3)$$

Where, G and  $T_a$  refers to the measured irradiance and array temperature, ‘ref’ refers to the reference conditions obtained from the  $P_{max}$  matrix, and ‘ $\gamma$ ’ refers to the temperature coefficient of power in (% / °C).

The total power generated by the array in a year is estimated by adding the instantaneous power obtained for that period.

The process is repeated for both the arrays under uniform and five shading scenarios using their respective  $P_{max}$  matrix obtained under these conditions.

**STEP X: Energy Yield and Performance Ratio Estimation and Comparison**

The output performance of S-S and TCT-S arrays have been assessed and compared on the basis of their energy yield and performance ratio under unshaded and five different shading scenarios. For the comparative purpose, normalized rating of 1kW for both the arrays has been considered.

**Energy yield** of the array under any condition of uniform irradiance or partial shaded condition is estimated from the sum of the calculated instantaneous power obtained under the same condition, using equation (4) given below

$$E_o = \Delta t \times \sum P_{oi} \quad (4)$$

Where:

$E_o$  = Energy output of the array (Wh)

$\Delta t$  = data sampling interval (= 10 min.)

$P_{oi}$  = Instantaneous power output of the array at the  $i^{th}$  sample time (W)

**Performance ratio (PR)** is the ratio of measured output to expected output for a given period based on the system name-plate rating and is calculated according to the equation (5) given below [46]:

$$PR = \frac{(E_o/P_{STC})}{(H_i/G_{STC})} \quad (5)$$

Where,

$E_o$  = energy output (D.C) from the PV system in kWh.

$P_{STC}$  = array power rating (D.C) at Standard Test conditions, in kW.

$H_i$  = total in-plane irradiation in kWh/m<sup>2</sup>.

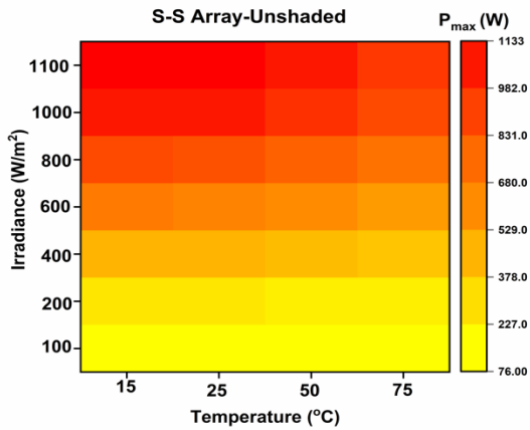
$G_{STC}$  = 1000  $W/m^2$

**3. Results and discussion**

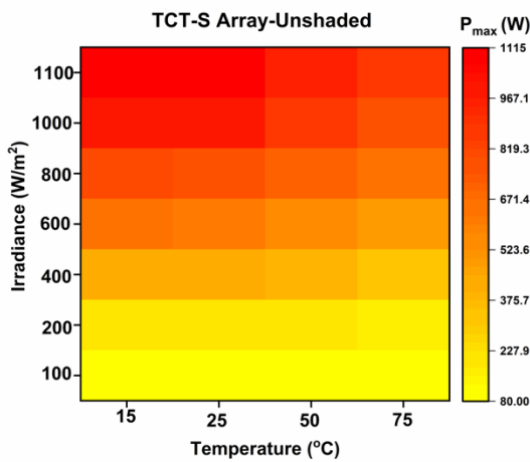
**3.1 For Unshaded Outdoor Condition**

From the outdoor measurements conducted on both the arrays, power matrix composed of 22 average values of  $P_{max}$  as a function of irradiance and temperature as per standard IEC 61853-1 is constructed. The remaining 06 conditions have been estimated using translation procedure one of IEC 60891 [47]. Surface plot representing the variation of  $P_{max}$  with irradiance and temperature is shown in Fig. 4. The obtained values of  $P_{max}$  for S-S array ranges from 76 W to 1133 W, while for TCT-S array it is from 80 W to 1115 W. Using the obtained  $P_{max}$  matrix and the method described earlier, the energy yield and DC performance ratio estimation for one complete year is presented in Table 3. The estimated annual energy yield for S-S and TCT-S array is 1539.4 kWh/kW and 1529.5 kWh/kW respectively under no shadow condition. The

DC performance ratio estimated for S-S and TCT-S array for one complete year is 92.8 % and 92.3 % respectively under no shadow condition.



(a)



(b)

**Fig. 4.** Surface plot showing the variation of  $P_{max}$  with irradiance and temperature under unshaded conditions for (a) S-S and (b) TCT-S array.

**Table 3.** Energy generation and performance ratio of array of 1kW each of S-S and TCT-S configuration for a year under unshaded condition.

Annual Energy Generation (kWh) under unshaded condition		Performance Ratio under unshaded condition	
S-S	TCT-S	S-S	TCT-S
1539.4	1529.5	0.928	0.923

3.2 Under Shaded Condition

The annual energy yield estimation of both the arrays under each shading condition occurring throughout the year is presented in Table 4.

**Table 4.** Annual energy yield generation and performance ratio of array of 1kW each of S-S and TCT-S configuration under different shaded scenarios.

Shading scenario	Annual Yield under conditions	Energy (kWh) under shading	Performance Ratio under shading conditions	
	S-S array	TCT-S array	S-S array	TCT-S array
Scenario-1	656.4	858.3	0.39	0.52
Scenario-2	773.5	1330.2	0.47	0.80
Scenario-3	1039.3	1193.6	0.63	0.72
Scenario-4	990.8	1048.4	0.59	0.63
Scenario-5	1081.2	1414.7	0.65	0.85

The comparative annual energy yield for both the arrays under unshaded and different shading scenarios has been presented in the form of bar graphs in Fig. 5. It is seen clearly from the results that under the shading scenarios the output energy as well as the annual PR of conventional S-S array is drastically reduced. However, the impact of shadings on the energy yield of TCT-S configuration of PV array is much less in comparison to S-S array, and has better performance ratio. Of all the shading scenarios considered, scenario-1 has the most pronounced effect on the performance of S-S, resulting in a loss of 57.4 % of annual energy yield. However, the impact of same shading scenario

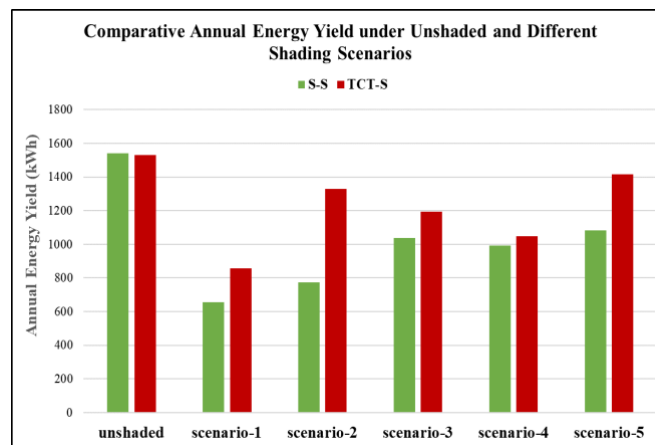


**Fig. 5.** Comparative annual energy yield of TCT-S array w.r.t S-S array under unshaded and different shading scenarios.

on TCT-S array resulted in a reduced loss of 43.9 % in the annual energy yield. Shading scenario-2 has the second most impact on the performance of S-S array, resulting in 49.8 % loss in annual energy yield which is reduced to merely 12.9 % in case of TCT-S array. It is found that of all the shading scenarios considered, the least adverse effect is produced by shading scenario-5 on both the arrays. However, it still causes 29.4 % loss in the annual energy yield of the S-S array and just 7.5 % for TCT-S array. The comparative annual energy loss of both the arrays under all the shading scenarios is presented in Fig. 6.

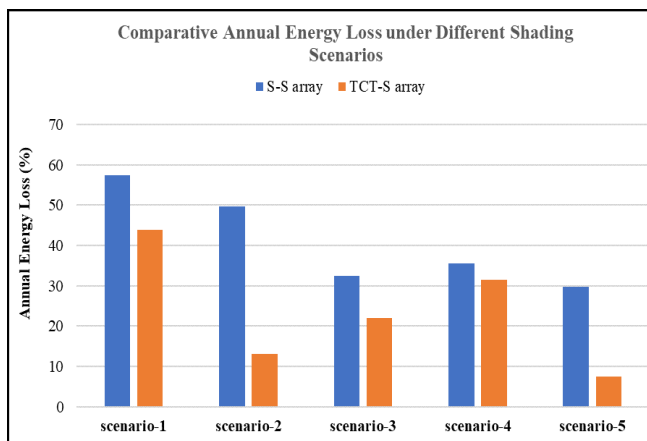


**Fig. 6.** Annual energy loss (%) suffered by S-S and TCT-S array under different shading scenarios.

Annual energy yield enhancement achieved by TCT-S array w.r.t S-S array under different shading scenarios is presented in Fig. 7. TCT-S array enhances the energy output under all shaded conditions, though the percentage of enhancement is different for different shading scenarios.

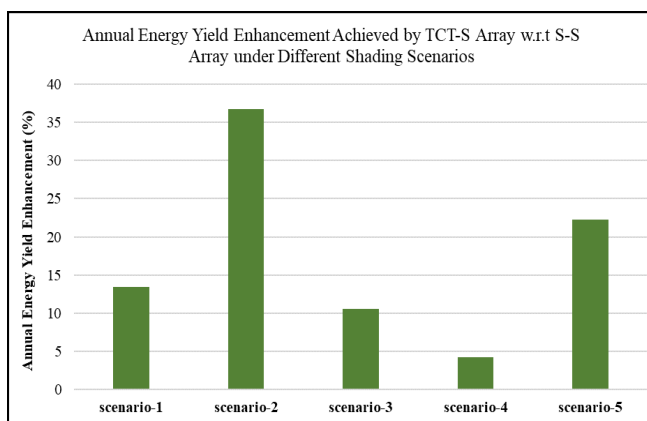


**Fig. 7.** Annual energy yield enhancement achieved by TCT-S array w.r.t S-S array under different shading scenarios.

#### 4. Uncertainty Analysis

The uncertainty in the estimation of PV array output power experimentally has been evaluated using the international ‘Guidelines of Uncertainty in Measurement’ (GUM) [48]. In this study, all the outdoor measurements of PV modules were done by portable Solmetric PV Analyzer. The various sources of uncertainty that have been considered to estimate the combined uncertainty in the measured output power of a module is presented in Table 5.

**Table 5.** Uncertainty components taken into consideration in estimating overall uncertainty in measured output PV array power.

Component	Standard uncertainty
Current measurement	$\pm 0.0157$ A
Voltage measurement	$\pm 0.0065$ V
Resolution of the current readings	$\pm 0.00058$ A
Resolution of the voltage readings	$\pm 0.0072$ V
Uncertainty in maximum current due to temperature	$\pm 0.0065$ A
Uncertainty in maximum voltage due to temperature	$\pm 0.0148$ V
Uncertainty in maximum current due to irradiance	$\pm 0.1374$ A

The estimated total expanded uncertainty in the power measurement is  $\pm 3.32$  % with a confidence level of 95 % and coverage factor  $k = 2$ .

#### 5. Cost Implication

A TCT-module differ from conventional S-module only in terms of interconnection scheme of constituent solar cells. Therefore, the additional cost in manufacturing TCT module comes from the additional length of PV ribbons used in making cross-ties, which adds only insignificantly to the existing cost of manufacturing conventional modules. The certified module manufacturing company who did the task of manufacturing TCT modules also informed that no significant additional cost and labour would be required in mass manufacturing of these modules. However, while performing the experiments, it was observed that in a TCT configuration there is an enhancement of current in comparison to the conventional, which can increase the resistive wiring losses. Therefore, as an engineering trade-off, copper wires of thicker cross-section need to be used.

#### 6. Conclusion

In the presented work, we have investigated the comparative effect of long term-partial shading conditions on the energy yield and DC performance ratio of the proposed TCT-S and conventional S-S configurations of PV array. The TCT-S configuration generates almost same energy and has same DC performance ratio as conventional array under uniform irradiance condition or no shading condition. But under PS conditions, the advantage of TCT-S array over S-S array is evident. The obtained results substantiate that under repeated partial shading conditions, PV array with conventional configuration (S-S) suffers greater energy yield loss. Proposed TCT-S configuration interconnections under same shading conditions generates more energy and has better performance ratio. Significant enhancement of annual energy yield ranging from 4.8 % to 36.7 % has been obtained by the TCT-S array over conventional array.

The results of this study are very significant especially for multi-storeyed complexes in urban areas places where it is highly probable that due to some surrounding structures/objects, the installed PV array gets partially shaded for large number of days in a year. Annual energy yield under partial shading can be enhanced by implementing the proposed configuration without any significant cost escalation, thereby benefitting the customers, PV industry and solar Project Developers.

Our future scope of work includes detail study of long-term performance of the proposed array taking into account the seasonal spectral variation and dynamic shadow conditions.

### Acknowledgement

The authors are grateful to administrative and technical staff at National Institute of Solar Energy (NISE), Gurgaon under Ministry of New and Renewable Energy (MNRE), Government of India, India for allowing us to use the facilities for conducting this experimental study.

### Funding

This research did not receive any specific grant from funding agencies in the public, commercial, or not-for-profit sectors.

### References

[1] K. Obaideen et al., "On the contribution of solar energy to sustainable developments goals: Case study on Mohammed bin Rashid Al Maktoum Solar Park," *International Journal of Thermofluids*, vol. 12, p. 100123, Nov. 2021, doi: 10.1016/J.IJFT.2021.100123.

[2] P. Moraitis, B. B. Kausika, N. Nortier, and W. van Sark, "Urban environment and solar PV performance: The case of the Netherlands," *Energies (Basel)*, vol. 11, no. 6, Jun. 2018, doi: 10.3390/en11061333.

[3] Owusu-Nyarko, K. H. Ahmed, F. Alsokhiry and Y. Al-Turki, "Grid Interfacing of Multi-megawatt Photovoltaic System under Normal and Partial Shading Conditions,"

2021 9th International Conference on Smart Grid (icSmartGrid), 2021, pp. 118-123, doi: 10.1109/icSmartGrid52357.2021.9551238.

[4] S. Hadji, L. Larbi, A. Belkaid, I. Colak and R. Bayindir, "Global optimum operating point tracker of PV system, under partial shading, using parallel searching," 2022 10th International Conference on Smart Grid (icSmartGrid), 2022, pp. 227-230, doi: 10.1109/icSmartGrid55722.2022.9848552.

[5] W. A. Abri, R. A. Abri, H. Yousef and A. Al-Hinai, "A Global MPPT Based on Bald Eagle Search Technique for PV System Operating under Partial Shading Conditions," 2022 10th International Conference on Smart Grid (icSmartGrid), 2022, pp. 325-332, doi: 10.1109/icSmartGrid55722.2022.9848561.

[6] D. Li, G. Liu, and S. Liao, "Solar potential in urban residential buildings," *Solar Energy*, vol. 111, pp. 225–235, Jan. 2015, doi: 10.1016/j.solener.2014.10.045.

[7] K. Brecl and M. Topič, "Self-shading losses of fixed free-standing PV arrays," *Renewable Energy*, vol. 36, no. 11, pp. 3211–3216, Nov. 2011, doi: 10.1016/j.renene.2011.03.011.

[8] R. Eke and C. Demircan, "Shading effect on the energy rating of two identical PV systems on a building façade," *Solar Energy*, vol. 122, pp. 48–57, Dec. 2015, doi: 10.1016/J.SOLENER.2015.08.022.

[9] M. Drif, A. Mellit, J. Aguilera, and P. J. Pérez, "A comprehensive method for estimating energy losses due to shading of GC-BIPV systems using monitoring data," *Solar Energy*, vol. 86, no. 9, pp. 2397–2404, Sep. 2012, doi: 10.1016/J.SOLENER.2012.05.008.

[10] X. Feng and T. Ma, "Solar photovoltaic system under partial shading and perspectives on maximum utilization of the shaded land," *International Journal of Green Energy*, pp. 1–12, Mar. 2022, doi: 10.1080/15435075.2022.2047977.

[11] K. Tsamaase, J. Sakala, E. Rakgati, I. Zibani and K. Motshidisi, "Solar PV Module Voltage Output and Maximum Power Yearly profile using Simulink-based Model," 2021 10th International Conference on Renewable Energy Research and Application (ICRERA), 2021, pp. 31-35, doi: 10.1109/ICRERA52334.2021.9598794.

[12] K. Brecl, M. Bokalič, and M. Topič, "Annual energy losses due to partial shading in PV modules with cut wafer-based Si solar cells," *Renewable Energy*, vol. 168, pp. 195–203, May 2021, doi: 10.1016/j.renene.2020.12.059.

[13] J. Solis, A. Råberg, J. André and M. Nilsson, "Analyzing the effect of snow in PV regulator response in a PV solar park," 2021 9th International Conference on Smart Grid (icSmartGrid), 2021, pp. 72-75, doi: 10.1109/icSmartGrid52357.2021.9551233.

[14] N. Agrawal, B. Bora, and A. Kapoor, "Experimental investigations of fault tolerance due to shading in photovoltaic modules with different interconnected solar

- cell networks,” *Solar Energy*, vol. 211, 2020, doi: 10.1016/j.solener.2020.10.060.
- [15] N. D. Kaushika and N. K. Gautam, “Energy yield simulations of interconnected solar PV arrays,” *IEEE Transactions on Energy Conversion*, vol. 18, no. 1, pp. 127–134, 2003, doi: 10.1109/TEC.2002.805204.
- [16] N. D. Kaushika and A. K. Rai, “An investigation of mismatch losses in solar photovoltaic cell networks,” *Energy*, vol. 32, no. 5, pp. 755–759, 2007, doi: 10.1016/j.energy.2006.06.017.
- [17] L. Gao, R. A. Dougal, S. Liu, and A. P. Iotova, “Parallel-Connected Solar PV System to Address Partial and Rapidly Fluctuating Shadow Conditions,” *IEEE Transactions on Industrial Electronics*, vol. 56, no. 5, pp. 1548–1556, 2009, doi: 10.1109/TIE.2008.2011296.
- [18] M. Balato, L. Costanzo, and M. Vitelli, “Series–Parallel PV array re-configuration: Maximization of the extraction of energy and much more,” *Applied Energy*, vol. 159, pp. 145–160, Dec. 2015, doi: 10.1016/j.apenergy.2015.08.073.
- [19] B.S.S Santosh, M. Mohamed Thameem Ansari, P. Kantarao, A. Kapoor, and G. Kusuma, “Power Loss Analysis of Traditional PV Array Configurations Under Different Shading Conditions,” *International Journal of Renewable Energy Research*, vol. 12, No. 2, pp 1176–1203, June 2022.
- [20] S. Bana and R. P. Saini, “Experimental investigation on power output of different photovoltaic array configurations under uniform and partial shading scenarios,” *Energy*, vol. 127, pp. 438–453, 2017, doi: 10.1016/j.energy.2017.03.139.
- [21] F. Belhachat and C. Larbes, “Modeling, analysis and comparison of solar photovoltaic array configurations under partial shading conditions,” *Solar Energy*, vol. 120, pp. 399–418, Oct. 2015, doi: 10.1016/j.solener.2015.07.039.
- [22] O. Bingöl and B. Özkaya, “Analysis and comparison of different PV array configurations under partial shading conditions,” *Solar Energy*, vol. 160, pp. 336–343, Jan. 2018, doi: 10.1016/j.solener.2017.12.004.
- [23] S. R. Pendem and S. Mikkili, “Modelling and performance assessment of PV array topologies under partial shading conditions to mitigate the mismatching power losses,” *Solar Energy*, vol. 160, pp. 303–321, Jan. 2018, doi: 10.1016/j.solener.2017.12.010.
- [24] R. Ramaprabha and B. L. Mathur, “A comprehensive review and analysis of solar photovoltaic array configurations under partial shaded conditions,” *International Journal of Photoenergy*, vol. 2012. 2012. doi: 10.1155/2012/120214.
- [25] P. R. Satpathy, S. Jena, and R. Sharma, “Power enhancement from partially shaded modules of solar PV arrays through various interconnections among modules,” *Energy*, vol. 144, pp. 839–850, Feb. 2018, doi: 10.1016/j.energy.2017.12.090.
- [26] Y. J. Wang and P. C. Hsu, “An investigation on partial shading of PV modules with different connection configurations of PV cells,” *Energy*, vol. 36, no. 5, pp. 3069–3078, 2011, doi: 10.1016/j.energy.2011.02.052.
- [27] V. Jha and U. S. Triar, “A detailed comparative analysis of different photovoltaic array configurations under partial shading conditions,” *International Transactions on Electrical Energy Systems*, vol. 29, no. 6, 2019, doi: 10.1002/2050-7038.12020.
- [28] G. Sagar, D. Pathak, P. Gaur, and V. Jain, “A Su Do Ku puzzle based shade dispersion for maximum power enhancement of partially shaded hybrid bridge-link-total-cross-tied PV array,” *Solar Energy*, vol. 204, pp. 161–180, Jul. 2020, doi: 10.1016/j.solener.2020.04.054.
- [29] B. I. Rani, G. S. Ilango, and C. Nagamani, “Enhanced power generation from PV array under partial shading conditions by shade dispersion using Su Do Ku configuration,” *IEEE Transaction on Sustainable Energy*, vol. 4, no. 3, pp. 594–601, 2013, doi: 10.1109/TSTE.2012.2230033.
- [30] C. E. Ye, C. C. Tai, Y. P. Huang, and J. J. Chen, “Dispersed partial shading effect and reduced power loss in a PV array using a complementary SuDoKu puzzle topology,” *Energy Conversion Management*, vol. 246, 2021, doi: 10.1016/j.enconman.2021.114675.
- [31] P. Srinivasa Rao, P. Dinesh, G. Saravana Ilango, and C. Nagamani, “Optimal Su-Do-Ku based interconnection scheme for increased power output from PV array under partial shading conditions,” *Frontiers in Energy*, vol. 9, no. 2, 2015, doi: 10.1007/s11708-015-0350-1.
- [32] A. S. Yadav, R. K. Pachauri, Y. K. Chauhan, S. Choudhury, and R. Singh, “Performance enhancement of partially shaded PV array using novel shade dispersion effect on magic-square puzzle configuration,” *Solar Energy*, vol. 144, pp. 780–797, 2017, doi: 10.1016/j.solener.2017.01.011.
- [33] M. S. S. Nihanth, J. P. Ram, D. S. Pillai, A. M. Y. M. Ghias, A. Garg, and N. Rajasekar, “Enhanced power production in PV arrays using a new skyscraper puzzle based one-time reconfiguration procedure under partial shade conditions (PSCs),” *Solar Energy*, vol. 194, pp. 209–224, Dec. 2019, doi: 10.1016/j.solener.2019.10.020.
- [34] X. Gao, F. Deng, G. Wu, Q. Pan, C. Zheng, W. Wang, T. Cai, L. Jiang, “Divide and Conquer Q-Learning (DCQL) algorithm based Photovoltaic (PV) array reconfiguration scheme for alleviating the partial shading influence,” *Solar Energy*, vol. 249, pp. 21–39 Jan 2023, doi.org/10.1016/j.solener.2022.09.005.
- [35] A. M. Ajmal, T. Sudhakar Babu, V. K. Ramachandaramurthy, D. Yousri, and J. B. Ekanayake, “Static and dynamic reconfiguration approaches for mitigation of partial shading influence in photovoltaic arrays,” *Sustainable Energy Technologies and Assessments*, vol. 40, Aug. 2020, doi: 10.1016/j.seta.2020.100738.

- [36] F. Belhachat and C. Larbes, "PV array reconfiguration techniques for maximum power optimization under partial shading conditions: A review," *Solar Energy*, vol. 230. Elsevier Ltd, pp. 558–582, Dec. 01, 2021. doi: 10.1016/j.solener.2021.09.089.
- [37] K. Osmani, A. Haddad, H. Jaber, T. Lemenand, B. Castanier, and M. Ramadan, "Mitigating the effects of partial shading on PV system's performance through PV array reconfiguration: A review," *Thermal Science and Engineering Progress*, vol. 31, p. 101280, Jun. 2022, doi: 10.1016/J.TSEP.2022.101280.
- [38] D. S. Pillai, J. P. Ram, V. Shabunko, and Y. J. Kim, "A new shade dispersion technique compatible for symmetrical and unsymmetrical photovoltaic (PV) arrays," *Energy*, vol. 225, 2021, doi: 10.1016/j.energy.2021.120241.
- [39] S. Reza zadeh, A. Moradzadeh, K. Pourhossein, M. Akrami, B. Mohammadi-Ivatloo, and A. Anvari-Moghaddam, "Photovoltaic array reconfiguration under partial shading conditions for maximum power extraction: A state-of-the-art review and new solution method," *Energy Conversion Management*, vol. 258, p. 115468, Apr. 2022, doi: 10.1016/J.ENCONMAN.2022.115468.
- [40] G. Sai Krishna and T. Moger, "A novel adaptive dynamic photovoltaic reconfiguration system to mitigate mismatch effects," *Renewable and Sustainable Energy Reviews*, vol. 141, May 2021, doi: 10.1016/j.rser.2021.110754.
- [41] N. Agrawal, B. Bora, S. Rai, A. Kapoor, and M. Gupta, "Performance Enhancement by Novel Hybrid PV Array Without and With Bypass Diode Under Partial Shaded Conditions: An Experimental Study," *International Journal of Renewable Energy Research*, vol. 11, No. 4, pp 1880-1891, December 2021.
- [42] N. Agrawal, A. Kapoor, and M. Gupta, "Monthly energy yield assessment of solar photovoltaic system under uniform irradiance and partial shaded condition," *Mater Today Proc*, vol. 68, pp. 2699–2704, Jan. 2022, doi: 10.1016/J.MATPR.2022.06.240.
- [43] G. Tamizhmani, K. Paghastian, J. Kuitche, M. Gupta, and V. G. Sivasubramanian, "Solar ABCs Policy Recommendations: Module Power Rating Requirements,," 2011. [Online]. Available: [www.solarabcs.org](http://www.solarabcs.org)
- [44] D. L. King, W. E. Boyson, and J. A. Kratochvil, "Photovoltaic array performance model," *Sandia Report No. 2004-3535*, vol. 8, 2004, doi: 10.2172/919131.
- [45] B. Durusoy, T. Ozden, and B. G. Akinoglu, "Solar irradiation on the rear surface of bifacial solar modules: a modeling approach," *Sci Rep*, vol. 10, no. 1, 2020, doi: 10.1038/s41598-020-70235-3.
- [46] IEC 61724, "IEC 61724 :Photovoltaic system performance monitoring - Guidelines for measurement, data exchange and analysis," no. February, 1998.
- [47] IEC 60891, "IEC 60891 INTERNATIONAL STANDARD Photovoltaic devices-Procedures for temperature and irradiance corrections to measured I-V characteristics," 2009.
- [48] Joint Committee for Guides In Measurements, "Evaluation of measurement data — Guide to the expression of uncertainty in measurement," *International Organization for Standardization Geneva ISBN*, vol. 50, no. September, 2008, doi: 10.1373/clinchem.2003.030528.